THE JOURNAL OF PHYSICAL CHEMISTRY B

Article

pubs.acs.org/JPCB

Development of Polarizable Models for Molecular Mechanical Calculations. 4. van der Waals Parametrization

Junmei Wang,[†] Piotr Cieplak,[‡] Jie Li,[§] Qin Cai,[∥] Meng-Juei Hsieh,[∥] Ray Luo,[∥] and Yong Duan*[,§]

[†]Department of Pharmacology, University of Texas Southwestern Medical Center at Dallas, 5323 Harry Hines Boulevard, Dallas, Texas 75390-9050, United States

[‡]Sanford-Burnham Medical Research Institute, 10901 North Torrey Pines Road, La Jolla, California 92037, United States

[§]Genome Center and Department of Biomedical Engineering, University of California at Davis, One Shields Avenue, Davis, California 95616, United States

[∥]Molecular Biology and Biochemistry, University of California at Irvine, 3144 Natural Sciences I, Irvine, California 92697-3900, United States

Supporting Information

ABSTRACT: In the previous publications of this series, we presented a set of Thole induced dipole interaction models using four types of screening functions. In this work, we document our effort to refine the van der Waals parameters for the Thole polarizable models. Following the philosophy of AMBER force field development, the van der Waals (vdW) parameters were tuned for the Thole model with linear screening function to reproduce both the *ab initio* interaction energies and the experimental densities of pure liquids. An in-house genetic algorithm was applied to maximize the fitness of "chromosomes" which is a function of the root-mean-square errors (RMSE) of interaction energy and liquid density. To efficiently explore the vdW parameter space, a novel approach was developed to estimate the liquid densities for a given vdW parameter set using the mean residue−residue interaction energies through interpolation/extrapolation. This approach allowed the costly molecular dynamics simulations be performed at the end of each optimization cycle only and eliminated the simulations during the cycle. Test results show notable improvements over the original AMBER FF99 vdW parameter set, as indicated by the reduction in errors of the calculated pure liquid densities (d), heats of vaporization (H_{vap}), and hydration energies. The average percent error (APE) of the densities of 59 pure liquids was reduced from 5.33 to 2.97%; the RMSE of H_{vap} was reduced from 1.98 to 1.38 kcal/mol; the RMSE of solvation free energies of 15 compounds was reduced from 1.56 to 1.38 kcal/mol. For the interaction energies of 1639 dimers, the overall performance of the optimized vdW set is slightly better than the original FF99 vdW set (RMSE of 1.56 versus 1.63 kcal/mol). The optimized vdW parameter set was also evaluated for the exponential screening function used in the Amoeba force field to assess its applicability for different types of screening functions. Encouragingly, comparable performance was observed when the optimized vdW set was combined with the Thole Amoeba-like polarizable model, particularly for the interaction energy and liquid density calculations. Thus, the optimized vdW set is applicable to both types of Thole models with either linear or Amoeba-like screening functions.

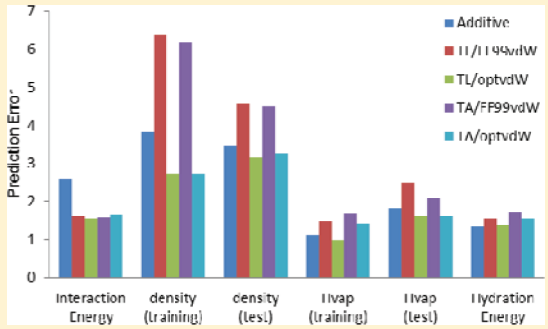

1. INTRODUCTION

With the growing computer power, there is an increasing desire to develop more accurate molecular mechanical models to study the structures, energies, and functions of biomolecules. To this end, various models that take into account the atomic polarization effect have been developed, including force fields that employ the induced dipoles such as OPLS/PFF,[1] AMOEBA,[2,3] and AMBER FF02, FF02EP,[4] and FF02r1.[5] Recently, we have developed a set of induced dipole models based on the Thole-screening approach to smooth out the surge of repulsion when two dipoles approach each other ("polarization catastrophe").[6,7] The Thole linear model, which has achieved the best overall performance in our tests, was selected as the base polarization model to parametrize other force field terms. A series of polarizable water models based on the Thole screening functions have also been developed recently.[8]

In the polarizable model, the nonbonded interactions comprise three integral components: electrostatic, polarization, and van der Waals forces. van der Waals (vdW) interaction is an important term in a molecular mechanical force field, and it is strongly coupled to the electrostatic energy term. For example, in some of the widely used force fields including CHARMM[9] and OPLS,[10] the vdW parameters and atomic

Received: February 29, 2012
Revised: May 9, 2012
Published: May 21, 2012

charges were tuned simultaneously. With the explicit inclusion of the induced dipoles in the energy function, it thus becomes necessary to refine the van der Waals terms to allow accurate representation of the nonbonded forces.

A major difference between AMBER and other force fields is that the atomic partial charges are derived to reproduce the *ab initio* molecular electrostatic potential (ESP) using a RESP approach. Thus, the atomic charges in AMBER are used for the purpose of representing the electrostatic potential that allows straightforward derivation of atomic charges.[11−14] Because the atomic charges are predetermined, the van der Waals parameters need to be tuned more thoroughly to reproduce high-level *ab initio* or high quality experimental data. This is also true in the polarizable model. Indeed, we found that our Thole polarizable model was unsatisfactory in reproducing the bulk properties with the vdW parameter set that was developed for the additive force fields (FF94,[11] FF99,[15] and FF03[13]) without adjustment. For a set of 25 pure liquids, the FF99 vdW parameter set has an average percent error (APE) of 6.37% for the densities and a root-mean-square error (RMSE) of 1.47 kcal/mol for the heats of vaporization (H_{vap}), respectively. Compared to the FF99/GAFF[14] additive model, the prediction errors of densities and heats of vaporization were increased 66 and 32%, respectively. The objective of this work is to develop a set of van der Waals parameters in conjunction with our Thole polarizable model to reproduce high level *ab initio* and high quality experimental data.

In AMBER force fields, the van der Waals term is described by the Lennard-Jones 6-12 potential (eq 1). A_{ij} and B_{ij}, the Lennard-Jones parameters for repulsion and attraction, can be expressed in terms of effective van der Waals radii and well depths, R_{ij}^* and ε_{ij} (eqs 1b and 1c), which are further obtained from atomic parameters using the Lorentz−Berthelot mixing rules (eqs 1d and 1e), R_{ij} is the distance between atoms i and j.

$$V_{vdW} = \sum_{i<j}\left[\frac{A_{ij}}{R_{ij}^{12}} - \frac{B_{ij}}{R_{ij}^{6}}\right] \tag{1a}$$

$$A_{ij} = \varepsilon_{ij}(R_{ij}^*)^{12} \tag{1b}$$

$$B_{ij} = 2\varepsilon_{ij}(R_{ij}^*)^{6} \tag{1c}$$

$$R_{ij}^* = R_i^* + R_j^* \tag{1d}$$

$$\varepsilon_{ij} = \sqrt{\varepsilon_i \varepsilon_j} \tag{1e}$$

The Lennard-Jones 12-6 potential is widely used by many force fields, which include CHARMM,[9] OPLS,[10] GROMOS,[16] UFF,[17] etc. Other popular vdW potentials include the "soft" Lennard-Jones 9-6 potential[18,19] and the buffered 14-7 potential,[20] among others.

van der Waals parametrization is regarded as one of the most difficult parts in the development of a molecular mechanical force field. This is particularly true for the general purpose force fields that have broad coverage of the elements, such as UFF,[17] ESFF,[19] and MMFF.[20] For the general-purpose force fields, the vdW parameters are usually obtained using empirical functions. In these force fields, the radii and well depths are expressed as functions of ionization energy, electronegativity, hardness, atomic polarizability, and Slater−Kirkwood effective numbers of valence electrons.[20] For force fields focused on studying biological systems, as is the case in this work, the van der Waals parameters are usually derived to reproduce liquid phase properties. OPLS[10] and COMPASS[18] belong to this group. For AMBER,[11−13] CHARMM,[9] and GROMOS,[16] the van der Waals parameters are also refined to reproduce liquid state properties such as densities and heats of vaporization.

There are two complementary approaches in the parametrization of van der Waals parameters. One approach is purely based on condensed phase properties. However, such an approach may suffer from a parameter correlation problem. For example, Kaminski et al. found that the standard OPLS-AA greatly overestimates the gas phase dimerization energies of methanethiol and ethanethiol, although their liquid state properties are in very good agreement with the experimental results.[21] Alternatively, vdW parametrization can also be based on *ab initio* data. However, vdW parameters developed solely on the basis of *ab initio* data could also be problematic, as suggested in many studies.[22,23] We also found that adjusting van der Waals parameters can notably improve the interaction energies of the first 673 dimers in Table S1 in the Supporting Information to achieve respectable results with AUE and RMSE reduced to 0.69 and 1.30 kcal/mol, respectively. Unfortunately, the vdW parameter set obtained this way resulted in a notable increase in the densities of 25 pure liquids with an average 14% difference from the experimental values. Therefore, a better strategy of vdW parametrization should utilize both the *ab initio* and experimental data in parametrization.

However, it is a challenging endeavor to design a parametrization protocol to efficiently obtain the data of liquid properties that are typically calculated through molecular simulations. Yin and Mackerell proposed an iterative two-staged procedure to conduct vdW parametrization.[23] In their approach, the *ab initio* interaction energies and geometries are used to optimize the relative magnitude of the vdW parameters. In the second step, the absolute values of the vdW parameters were tuned to reproduce experimental densities and H_{vap} of pure liquids. Their approach has been applied to produce vdW parameters and atomic charges for single molecular classes.[23−25]

In this work, we set out to conduct vdW parametrization for the Thole polarizable model to reproduce both high level quantum mechanically derived interaction energies and experimental pure liquid densities using a genetic algorithm. As in a typical GA run, the fitness functions are evaluated more than 100 000 times and it is impractical for us to calculate the densities through molecular simulations during the GA optimization. To tackle this problem, a novel approach is developed to predict the liquid densities from the mean residue−residue interaction energies through interpolation and extrapolation. The final vdW parameter set optimized by GA was thoroughly evaluated in predicting three condensed phase properties including densities, heats of vaporization, and hydration energies, for 59 small molecules through molecular dynamics simulations.

2. METHODS

In this section, we first discuss how to conduct van der Waals parametrization to reproduce both the *ab initio* interaction energies and experimental liquid densities. Then, the MD simulation protocols and an approach to calculate liquid properties are discussed sequentially.

2.1. van der Waals Parameterization. In this work, we propose to predict the liquid densities for an arbitrary vdW set

dx.doi.org/10.1021/jp3019759 | J. Phys. Chem. B 2012, 116, 7088−7101

using the mean residue−residue interaction energies. The procedure of vdW parametrization is summarized in Figure 1.

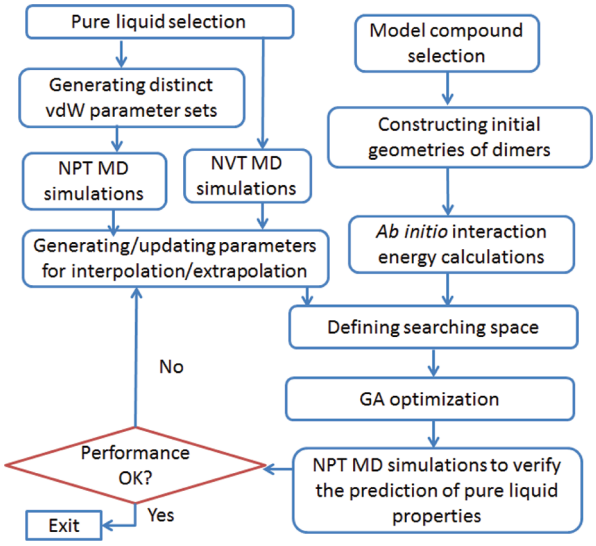

Figure 1. Procedure of van der Waals parametrization.

Before the GA optimization, two types of data need to be prepared. The first type of data includes quantum mechanically derived interaction energies for a set of model compounds that best represent the vdW. In this work, the model compounds are typically the building blocks of amino acids and nucleic acids.

The second type of data is used to predict the densities of pure liquids. For each liquid, a constant volume MD simulation is performed to produce a NVT (canonical) ensemble, and the density of the simulation box is set to the experimental value. Second, two distinct vdW parameter sets are generated and constant pressure MD simulations are performed for both vdW parameter sets for each liquid. The densities of liquid i, d_i^1 and d_i^2, corresponding to the two vdW parameter sets are obtained from the NPT simulations. Ideally, the experimental density d_i is between d_i^1 and d_i^2. The mean intermolecular interaction energies of the two vdW parameter sets, E_i^1 and E_i^2, are also calculated using the last snapshot of the NVT MD simulation. The mean intermolecular interaction energy E is calculated by eq 2

$$E = (E_{\mathrm{mol}} - \sum_{j=1}^{n} E_{\mathrm{res}}^{j})/n \tag{2}$$

where E_{mol} is the energy of the entire system, E_{res}^{j} is the intramolecular potential energy of the jth residue, and n is the number of molecules in the simulation box. Here, a solvent molecule is often a single residue in a pure solvent system.

Rather than running MD simulations to calculate densities, we predict this property through interpolation and extrapolation. For an arbitrary vdW parameter set, mean intermolecular interaction energy of liquid i, E_i, can be easily calculated using eq 2, and its density can be predicted through interpolation/extrapolation using eq 3:

$$d_i = d_i^1 + (d_i^2 - d_i^1) \times \frac{E_i - E_i^1}{E_i^2 - E_i^1} \tag{3}$$

It should be noted that the linear relationship of eq 3 holds only when d_i^1 and d_i^2 are close to the experimental value d_i. In practice, the van der Waals parameters are refined iteratively and the parameters that fail to make satisfactory prediction should be replaced with new ones.

An in-house generic algorithm (GA) is applied to optimize vdW parameters to maximize the fitness function (eq 4) which measures the performance of a vdW parameter set in reproducing the *ab initio* interaction energies and experimental densities of pure liquids simultaneously.

$$f = w_{\mathrm{IE}} \frac{1}{\mathrm{RMSE}_{\mathrm{IE}} + 0.001} + w_{\mathrm{d}} \frac{1}{\mathrm{APE}_{\mathrm{d}} + 0.001} \tag{4}$$

In eq 4, w_{IE} and w_{d} are adjustable parameters balancing the relative importance of the two properties, interaction energy and density; $\mathrm{RMSE}_{\mathrm{IE}}$ is the root-mean-square error of the interaction energy calculation and $\mathrm{APE}_{\mathrm{d}}$ is the average percent error of the density prediction; 0.001 is added to avoid possible numerical overflow. In this work, w_{IE} and w_{d} are set to 1.2 and 2.0, respectively. When $\mathrm{RMSE}_{\mathrm{IE}}$ approaches 1.2 kcal/mol and $\mathrm{APE}_{\mathrm{d}}$ approaches 2.0%, the two properties contribute equally to the fitness.

Although GA optimization is an automatic procedure, human intuition is needed to adjust the GA searching ranges and redefine atom types. The parametrization procedure is an iterative procedure, and a satisfactory vdW parameter set may be obtained only after several GA runs. More details on the algorithm and parameter setting for GA optimization can be found in other publications.[6,26−28]

2.2. Data Sets. *Interaction Energies.* In this work, a total number of 1639 dimers were studied and those dimers fall into one of seven categories: (1) amino acid main chain analogue dimers, (2) amino acid side chain analogue dimers, (3) water−amino acid analogue dimers, (4) hydrogen-bonded nucleic acid base pairs, (5) stacked nucleic acid base pairs, (6) nucleic acid base steps, and (7) diverse pairs representing various interaction types.

All the entries of set 1 are actually the NMA (*N*-methylacetamide) dimers. The first 31 entries (nos. 1−31) were taken from our previous publication.[7] For nos. 32−64, the intermolecular distances d between two atoms were constrained during the geometry optimization. Specifically, d are the distances between two amine hydrogen atoms for nos. 32−44, the distances between amine hydrogen and carbonyl oxygen for nos. 45−56, and the distances between two carbonyl oxygen atoms for nos. 57−64. The exact values of separation distances are indicated by the entry names. For nos. 65−85, the NMA dimers were generated in the same fashion as already reported except that smaller separation distances were applied.[7] Again, the separation distances are indicated by the entry names. In set 2, entry nos. 536−602 are newly added dimers and the others come from the previous study.[7] We added those entries because some interaction types (polar−polar and aromatic−aromatic interactions) were somehow under-represented in the initially chosen set of dimers (nos. 86−535). Again, the same protocol was used to construct the geometries of newly introduced entries. In set 3, 71 dimers were constructed representing water and amino acid analogue interactions. A similar protocol to the one proposed in ref 7 was used to generate the geometries of dimers. In brief, dimers that frequently occur in protein crystal structures were selected and clustered, and the representative structures from the top clusters were then selected for *ab initio* calculations. More details on raw water dimer generation and cluster analysis are presented in our previous work.[7]

dx.doi.org/10.1021/jp3019759 | J. Phys. Chem. B 2012, 116, 7088−7101

The newly added entries in sets 1−3 were optimized at the MP2/6-311++G(d,p) level. The optimization details on the other entries (nos. 1−31 and 86−535) were described in previous work.[7] Single point calculations at the MP2/aug-cc-pVDZ (in abbreviation aDZ) and MP2/aug-cc-pVTZ (in abbreviation aTZ) levels were performed for all the 673 dimers. The basis set superposition errors (BSSE) were corrected through the counterpoise corrections.[29,30] The interaction energies extrapolated to the complete basis set (CBS) level were calculated using four interaction energies: BSSE corrected interaction energy at the aDZ level (ΔE_{aDZ}^{BSSE}), BSSE corrected interaction energy at the aTZ level (ΔE_{aTZ}^{BSSE}), interaction energy at the aDZ level (ΔE_{aDZ}), and interaction energy at the aTZ level (ΔE_{aTZ}) using a scheme proposed by Truhlar et al.[31,32] All of these four interaction energies were calculated by subtracting the monomer energies from the dimer energy computed using the same quantum mechanical model.

Set 4 (nos. 674−702) come from Šponer, Jurecka, and Hobza's work.[33] Intermolecular hydrogen bonds formed for dimers in this set and their interaction energies were also extrapolated using aDZ and aTZ energies. Set 5 (nos. 703−948) contains stacked adenine[34] and uracil pairs.[35] The interaction energies were calculated by extrapolating the aDZ and aTZ energies plus higher-order correlation energy calculated at the CCSD(T) level using a small basis set. Set 6 (nos. 949−1048) comes from Svozil, Hobza, and Šponer's work on intrinsic stacking energy calculation for dinucleotide steps in A-RNA and B-DNA duplexes.[36] The interaction energies were calculated using the RI-MP2 complete basis set limit method augmented with the CCSD(T) correction term derived with a smaller basis set. Set 7 (nos. 1049−1639) contains 66 molecular complexes representing different types of interactions. For each complex, the interaction energies at equilibrium geometry and dissociation curve were calculated at the CCSD(T)/CBS level. All the geometric and energetic data come from the recent work of Řezáč, Riley, and Hobza.[37]

Condensed Phase Properties. In total, the molecular properties of 59 compounds were studied in this work. Those compounds cover diverse functional groups in organic chemistry, which include hydrocarbons (aliphatic and aromatic, cyclic and acyclic), alcohols, thiol, phenols, ethers, esters, aldehydes, ketones, carboxylic acids, amines, amides, nitriles, nitro-derivatives, disulfides, thiophenes, sulfides, sulfoxides, sulfones, phosphates, halides, and heterocyclic compounds. The experimental densities and heats of vaporization have already been cited in our recent work unless otherwise mentioned in Tables 7 and 8.[38] The following are additional data resources for densities and heats of vaporization: Jorgensen et al.,[39−42] Lide,[43] and Majer and Svoboda.[44] The experimental hydration free energies for 15 compounds in Table 6 come from our previous collection[45] and Mobley et al.'s work.[46] We divided the 59 compounds into two data sets: 25 compounds that are most relevant to the building blocks of amino acids and nucleic acids are placed in the training set to participate in van der Waals parametrization; the other 34 compounds in the test set are used to objectively evaluate the optimized van der Waals parameters.

2.3. Molecular Mechanical Models. Five molecular mechanical models, namely, the additive using FF99[15]/GAFF[14] (in abbreviation FF99/GAFF), two polarizable models with the FF99/GAFF vdW parameters (in abbreviation TL-FF99vdW and TA-FF99vdW), and two polarizable models with the optimized vdW parameters (in abbreviation TL-OptvdW and TA-OptvdW), were studied in this work. The functional forms of the two Thole polarizable models (TL and TA) are provided in the supporting text. For the additive model, the point charges were derived to fit the HF/6-31G* electrostatic potentials by the RESP program.[47] The charges of the four polarizable models were derived to fit the MP2/aug-cc-pVTZ electrostatic potentials by the i-RESP program.[48] Unlike RESP, the i-RESP program applies an iterative procedure to determine charges so that the ESP generated by the point charges plus ESP due to self-polarization reproduce the quantum mechanical ESP. The other force field parameters of the three molecular mechanical models come from FF99 and GAFF: whenever possible, the force field parameters in FF99 were adopted and the missing ones come from GAFF. Certainly, in the last two molecular mechanical models, the FF99/GAFF vdW parameters were substituted by the optimized ones.

All electrostatic potentials were generated using the Gaussian 03 software package.[49] The residue topology files were prepared using the Antechamber module[50] in AMBER 11.[51] For each molecule, an in house program was used to generate a rectangular parallelepiped box filled with multiple copies of the monomer, and then, the Leap program in AMBER11 was applied to generate the topology files.

2.4. Molecular Mechanical Calculations. An extended version of the Sander program in AMBER11 with implementation of the Thole screening functions was used to calculate the interaction energy and to perform minimizations and molecular dynamics simulations. The 1−4 van der Waals energies were scaled down by 50% for all the molecular mechanical calculations, while the 1−4 electrostatic energies were scaled down by a factor of 1/1.2 only for the additive model (FF99/GAFF). The 1−4 electrostatic scaling factor was set to 1.0 for the polarizable models (TL-FF99vdW, TL-OptvdW, TA-FF99vdW, and TA-OptvdW), consistent with the derivation of the charge sets.

The TIP3P water was applied in conjunction with FF99/GAFF, and two newly developed POL3 water models that are consistent with the Thole linear and Thole Amoeba-like models were used in conjunction with TL-FF99vdW/TL-OptvdW and TA-FF99vdW/TA-OptvdW, respectively.[8] Bond and bond angles in the additive and polarizable water were constrained with a special "three-point" algorithm.[52] Except where explicitly stated otherwise, all the degrees of freedom of other molecules were free to change in all the MD simulations.

The interaction energies in GA optimization were calculated using the *ab initio* geometries, and no cutoff was applied. In the control test of studying how minimization affects the interaction energy calculations using a subset of set 7, steepest descent and conjugated gradient minimizations were performed for each molecule until either the total cycles of minimization exceed 10 000 times or the root-mean-square of the gradient is less than 0.001 kcal/mol/Å.

All the liquid phase MD simulations were performed with the periodic boundary condition to produce either canonical or isothermal−isobaric ensembles using the *sander* program of AMBER11.[51] The particle mesh Ewald (PME) method[53−55] was used to calculate the full electrostatic energy of a unit cell in a macroscopic lattice of repeating images. The nonbonded cutoff of calculating van der Waals and electrostatic energies was set to 9.0 Å, and a continuum model correction term was added to the van der Waals energies. The effect of nonbonded cutoff on the MD simulations was discussed by Shirts et al.[56] Temperature was regulated using the Langevin dynamics[57] with

dx.doi.org/10.1021/jp3019759 | J. Phys. Chem. B 2012, 116, 7088−7101

Table 4. Densities of 25 Compounds in the Training Set (g/cm^3)

				additive	Thole-linear		Thole-Amoeba	
no.	compound	expt.	temp. (°C)	GAFF	FF99 vdW	Opt. vdW	FF99 vdW	Opt. vdW
1	isobutane	0.551	25	0.564 ± 0.004	0.587 ± 0.000	0.570 ± 0.000	0.587 ± 0.000	0.569 ± 0.000
2	trans-2-butene	0.598	25	0.546 ± 0.004	0.553 ± 0.000	0.575 ± 0.000	0.554 ± 0.001	0.575 ± 0.000
3	benzene	0.877	20	0.867 ± 0.006	0.877 ± 0.001	0.846 ± 0.001	0.875 ± 0.001	0.845 ± 0.000
4	ethanol	0.789	20	0.809 ± 0.006	0.856 ± 0.000	0.780 ± 0.001	0.867 ± 0.001	0.792 ± 0.000
5	acetic acid	1.045	25	1.120 ± 0.007	1.208 ± 0.002	1.134 ± 0.001		1.157 ± 0.001
6	methylamine	0.656	25	0.773 ± 0.007	0.818 ± 0.000	0.670 ± 0.000	0.826 ± 0.000	0.678 ± 0.000
7	*N*-methyl acetamide	0.894	100	0.901 ± 0.007	0.946 ± 0.001	0.910 ± 0.001	0.946 ± 0.000	0.909 ± 0.001
8	methanol	0.791	20	0.819 ± 0.007	0.854 ± 0.001	0.732 ± 0.001	0.865 ± 0.000	0.750 ± 0.001
9	phenol	1.055	45	1.051 ± 0.006	1.088 ± 0.001	1.063 ± 0.001	1.090 ± 0.001	1.065 ± 0.000
10	ethanethiol	0.832	25	0.824 ± 0.006	0.836 ± 0.000	0.825 ± 0.001	0.839 ± 0.000	0.827 ± 0.000
11	dimethyl ether	0.735	−24.6	0.754 ± 0.005	0.780 ± 0.000	0.747 ± 0.000	0.780 ± 0.000	0.747 ± 0.000
12	dimethyl sulfide	0.848	20	0.804 ± 0.006	0.845 ± 0.000	0.833 ± 0.001	0.845 ± 0.000	0.832 ± 0.000
13	acetone	0.785	25	0.787 ± 0.005	0.818 ± 0.000	0.793 ± 0.000	0.819 ± 0.000	0.792 ± 0.000
14	dimethyl amine	0.680	0	0.741 ± 0.005	0.758 ± 0.000	0.651 ± 0.001	0.761 ± 0.000	0.659 ± 0.000
15	trimethylamine	0.627	25	0.698 ± 0.005	0.752 ± 0.000	0.628 ± 0.000	0.750 ± 0.001	0.633 ± 0.000
16	aniline	1.022	20	1.074 ± 0.006	1.090 ± 0.001	1.066 ± 0.001	1.087 ± 0.001	1.069 ± 0.000
17	acetonitrile	0.786	20	0.731 ± 0.005	0.822 ± 0.000	0.786 ± 0.000	0.821 ± 0.000	0.786 ± 0.001
18	*N*,*N*-dimethyl acetamide	0.936	25	0.935 ± 0.005	0.965 ± 0.000	0.937 ± 0.001	0.966 ± 0.001	0.936 ± 0.000
19	dimethyl sulfoxide	1.101	25	1.126 ± 0.006	1.170 ± 0.000	1.159 ± 0.001	1.170 ± 0.000	1.159 ± 0.000
20	trichloromethane	1.479	25	1.448 ± 0.009	1.473 ± 0.001	1.428 ± 0.001	1.471 ± 0.001	1.429 ± 0.001
21	tetrachloromethane	1.594	20	1.607 ± 0.010	1.613 ± 0.001	1.577 ± 0.001	1.612 ± 0.001	1.574 ± 0.001
22	bromomethane	1.676	20	1.642 ± 0.013	1.666 ± 0.001	1.631 ± 0.001	1.664 ± 0.001	1.632 ± 0.001
23	tetrahydrofuran	0.883	25	0.891 ± 0.005	0.909 ± 0.001	0.864 ± 0.000	0.909 ± 0.001	0.864 ± 0.000
24	pyridine	0.982	20	0.992 ± 0.006	1.049 ± 0.000	1.016 ± 0.000	1.053 ± 0.001	1.020 ± 0.001
25	quinoline	1.098	15	1.105 ± 0.005	1.145 ± 0.000	1.128 ± 0.000	1.147 ± 0.000	1.131 ± 0.001
	average difference		0.012	0.046	0.001		0.043	0.004
	average percent difference		1.62%	5.66%	0.13%		5.44%	0.52%
	APE		3.83%	6.37%	2.70%		6.20%	2.73%
	AUE		0.031	0.051	0.026		0.049	0.026
	RMSE		0.042	0.067	0.033		0.062	0.035

a collision frequency of 5 ps.[58−60] Pressure regulation was achieved with isotropic position scaling, and the pressure relaxation time was set to 1.0 ps. For the additive model, the integration of the equations of motion was conducted at a time step of 2 fs, while, for the polarizable models, the time step was 1 fs and the convergence criterion of induced dipoles was set to 10^{-6} D.

There are three phases in a liquid phase MD simulation, namely, the relaxation phase, the equilibration phase, and the sampling phase. In the relaxation phase, the main chain atoms were gradually relaxed by applying a series of restraints and the force constants decreased progressively: from 20 to 10, 5, and 1.0 kcal/mol/Å^2. For each force constant, the position-restrained MD simulation was run for 20 ps. In the following equilibration phase, the system was further equilibrated for 2 ns without any restraints and constraints. For the NVT MD simulations, the dimensions of simulation boxes were adjusted so that the density is equal to the experimental value; then, the system was further equilibrated for another 3 ns. In the sampling phases of the NPT MD simulations, the snapshots as well as the structural and energy related properties were recorded at an interval of 1 ps, and in total, 1000 snapshots were saved for further analysis. For the NVT MD simulations, only 200 snapshots were sampled at an interval of 5 ps.

2.5. Molecular Property Calculations. *Density Calculations.* The average bulk density d was computed from the average volume of the simulation box, $\langle V \rangle$, using eq 5, where N_{res} is the number of residues in the simulation box, M is molar mass of the molecule in study, and N_A is the Avogadro constant. The bulk densities were printed out in the output files of MD simulations by *sander* in default.

$$\langle d \rangle = \frac{N_{res} M}{N_A \langle V \rangle} \tag{5}$$

Heat of Vaporization. The heat of vaporization ΔH_{vap} can be calculated with eq 6

$$\Delta H_{vap}(T) = E_{gas}^{potential}(T) - E_{liquid}^{potential}(T) + RT + C \tag{6}$$

$$E_{gas}^{potential}(T) = E_{gas}^{minimized} + \frac{1}{2}RT(3N_{atom} - 6 - N_{cons}) \tag{7}$$

where $E_{gas}^{potential}$ and $E_{liquid}^{potential}$ are the potential energies in the gas and liquid phases, respectively; $E_{liquid}^{potential}$ is obtained through molecular simulations, and $E_{gas}^{potential}$ is estimated using eq 7; $E_{gas}^{minimized}$ is the minimized energy in the gas phase; and N_{atom} and N_{cons} are the number of atoms in the molecules and the number of the constrained degrees of freedom, respectively. The correction term C in eq 6 accounts for the difference in vibration energies calculated quantum mechanically and classically, as well as for the polarization and nonideal gas effects. This term is small, and it is neglected in this work.

Solvation Free Energy Calculations. The vdW parameters of ions have been parametrized to reproduce the hydration energies.[61] However, solvation free energy is seldom applied to parametrize van der Waals terms of neutral molecules, even

dx.doi.org/10.1021/jp3019759 | J. Phys. Chem. B 2012, 116, 7088−7101

Table 1. List of the Optimized van der Waals Parameters

atom type	definition	radius (R)	well depth (ε)
H	hydrogen bonded to nitrogen other than HN1 and HN2	0.6000	0.0157
HN1	secondary amine hydrogen	0.8000	0.0100
HN2	primary amine hydrogen	1.0300	0.0100
HO	hydrogen bonded to oxygen	0.6000	0.0007
HS	hydrogen bonded to sulfur	0.6000	0.0157
HC	hydrogen bonded to sp^3 carbon	1.4164	0.0281
HA	hydrogen bonded to sp^2 and sp^1 carbon	1.5738	0.0060
H1	hydrogen bonded to sp^3 carbon with one electron-withdrawing group	1.3164	0.0281
H2	hydrogen bonded to sp^3 carbon with two electron-withdrawing groups	1.2164	0.0281
H3	hydrogen bonded to sp^3 carbon with three electron-withdrawing groups	1.1164	0.0281
H4	hydrogen bonded to sp^2 carbon with one electron-withdrawing group	1.5238	0.0060
H5	hydrogen bonded to sp^2 carbon with two electron-withdrawing groups	1.4738	0.0060
CT	sp^3 carbon	2.0085	0.0591
C	carbonyl carbon	1.9600	0.0623
CA, C*, CB, CC, CD, CK, CM, CQ, CR, CV, CW	aromatic sp^2 carbon or sp^2 carbon in planar ring systems	1.8807	0.1022
C2	other sp^2 carbon	1.8372	0.1354
CY	sp^1 carbon	1.9275	0.1859
OH	hydroxyl oxygen	1.8235	0.0301
OS	oxygen in ether and ester	1.6989	0.1526
O	carbonyl oxygen	1.6600	0.1831
O2	carboxyl and phosphate oxygen	1.4000	1.4722
N, NA, N2, N*, NC, NB, NY	nitrogen other than NT and N3	1.8600	0.1345
NT, N3	amine nitrogen	1.9000	0.0500
S, SH	sulfur	1.9901	0.2653
P	phosphate	2.2286	0.0980

though it is a standard practice to test if a molecular mechanical model is capable of reproducing the experimental solvation free energies of model compounds.

The hydration free energy of a molecule was calculated using thermodynamic integration (TI). In TI calculations, the system evolves according to a mixed potential, $V(\lambda) = (1 - \lambda)^k V_0 + [1 - (1 - \lambda)^k]V_1$, where λ and k are mixing parameters and V, V_0, and V_1 are the mixed, unperturbed, and perturbed potentials, respectively. The free energy change, ΔG, is calculated numerically using eq 8.

$$\Delta G = G_{\lambda=1} - G_{\lambda=0} = \int_0^1 \langle \partial V/\partial\lambda \rangle_\lambda \, d\lambda = \sum_i w_i \langle \partial V/\partial\lambda \rangle_i \tag{8}$$

The solvation free energy of a molecule was calculated by summing up the free energy changes in four perturbations, i.e., the gas-phase and aqueous-phase disappearing of Coulombic interactions and the gas-phase and aqueous-phase disappearing of the van der Waals interactions. For the disappearing of Coulombic interactions, a linear mixing rule was applied (k = 1); for the disappearing of the van der Waals interactions, k was set to 6, as suggested by Steinbrecher et al.[62] For each of the four free energy perturbations (two in gas phase and two in aqueous solution), nine windows/free energy simulations were performed in order to numerically estimate the integral in eq 8. The free energy change of the ith window $\langle \partial V/\partial\lambda \rangle_i$ was weighted by w_i. The weight parameters w_i, which were obtained to fit the Gaussian quadrature formula, came from ref 62. Except that the systems were equilibrated for 1 ns followed by production for another nanosecond and the bonds involving hydrogen were constrained, the other MD setting is the same as the pure liquid MD simulations discussed above.

Statistical Uncertainty Estimation. The density and most energetic terms in heat of vaporization calculations are ensemble averages. The uncertainty of a term (densities, temperatures, and energies) was estimated by the rms deviation of a serial of accumulated means. For each property, the means were calculated using the first 500, 525, 550, 575, 600, ..., 1000 snapshots.

For the hydration energies, the uncertainty of free energy change in each simulation was calculated in a similar way. To calculate the uncertainty of a free energy component, such as charging in the aqueous phase, the weighted uncertainties of nine simulations were summed up. The uncertainty of the hydration energy of a compound was obtained by summing up the uncertainties of four free energy components (charges and vdW parameters disappearing in both gas and aqueous phases).

3. RESULTS AND DISCUSSION

In this section, we first present the efficiency of our iterative procedure in van der Waals parametrization and then discuss the performance of the optimized vdW parameter set in calculating the interaction energies and condensed-phase molecular properties.

3.1. van der Waals Parameterization Using a Genetic Algorithm. As mentioned in the Methods section, the van der Waals parametrization was performed with the Thole linear polarizable model and the optimized vdW set was also evaluated by the Thole Amoeba-like polarizable model. Atomic coordinates and interaction energies for the 1639 dimers, required for the GA optimization, were derived using high level *ab initio* models. Twenty-five pure liquids (see Tables 4 and 5) were selected for density prediction. For each liquid, 200 snapshots were obtained from constant volume MD simulations using the FF99/GAFF model. The last snapshot (MD Frame 200) was used to calculate the residue−residue interaction energies for any arbitrary vdW parameter set. It is emphasized that the most time-consuming part of GA

dx.doi.org/10.1021/jp3019759 | J. Phys. Chem. B 2012, 116, 7088−7101

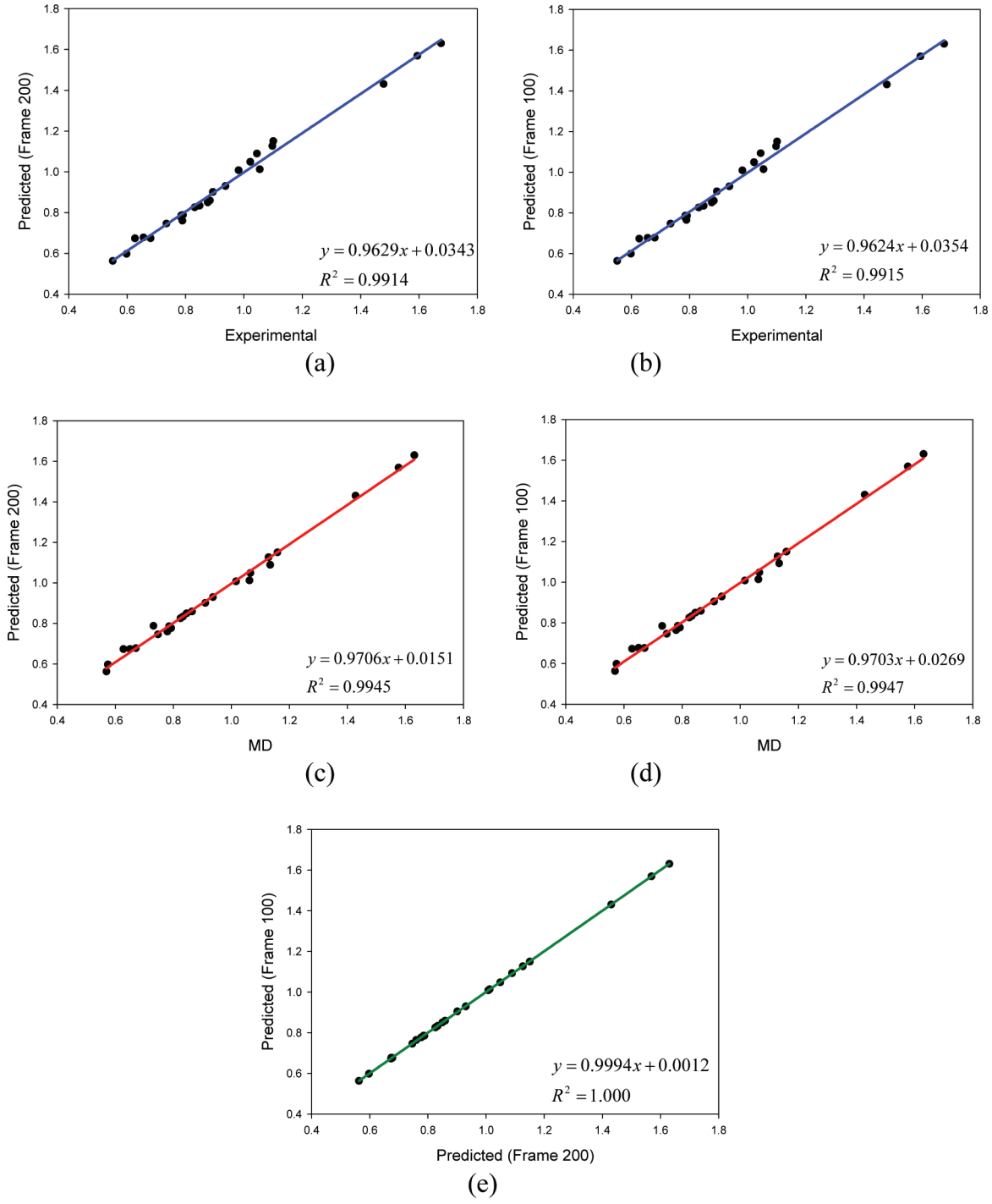

Figure 2. Comparison of predicted densities (in g/cm^3) by TL/OptvdW: (a) experimental versus predicted using MD Frame #200, (b) experimental versus predicted using MD Frame #100, (c) MD densities versus predicted using MD Frame #200, (d) MD densities versus predicted using MD Frame #100, and (e) predicted densities using MD Frames #100 and #200.

optimization is to calculate the mean residue−residue interaction energies; therefore, only one NVT snapshot (MD Frame #200) was used in density prediction. The further justification of using one NVT snapshot will be provided below.

Two distinct vdW parameter sets were needed to interpolate/extrapolate the parameters. Ideally, one vdW set overestimates and the other underestimates the densities of the selected liquids. Since the FF99 vdW set overestimates the densities for most liquids in the training set, it was selected as the first vdW set. To prepare the other vdW set, we adjusted the radii and well depths to scale down the "*B*" parameters in eq 1a by 10% while keeping the "*A*" parameters unchanged. This vdW parameter set is referred to as the B90 set. As the attraction energies were scaled down, it is expected that the densities predicted by B90 are underestimated. In a few cases where even the B90 set overestimates the densities, the B90 set was replaced with another vdW set which can underestimate the densities. The residue−residue interaction energies were initially calculated for these two distinct vdW parameter sets. The parameters used in density prediction are listed in Table

dx.doi.org/10.1021/jp3019759 | *J. Phys. Chem. B* 2012, 116, 7088−7101

Table 2. Performance of Three Molecular Mechanical Models in Interaction Energy Calculations (kcal/mol)

				Thole-linear				Thole-Amoeba			
		additive		FF99vdW		Opt. vdW		FF99vdW		Opt. vdW	
dimer class	#data	AUE	RMSE	AUE	RMSE	AUE	RMSE	AUE	RMSE	AUE	RMSE
amino acid main chain analogue dimers	85	0.70	1.18	0.37	0.64	0.42	0.71	0.37	0.62	0.42	0.70
amino acid side chain analogue dimers	517	2.61	4.09	1.42	1.97	1.31	1.79	1.37	1.86	1.39	2.02
water amino acid analogue dimers	71	1.33	2.02	1.31	2.26	1.26	1.94	1.34	2.28	1.38	2.12
hydrogen-boned nucleic base pairs	29	1.53	2.14	1.73	2.10	1.62	2.02	1.78	2.19	1.69	2.09
stacked nucleic base pairs	246	1.27	2.10	1.29	1.90	1.25	2.06	1.29	1.89	1.25	2.06
nucleic acid base steps	100	0.85	1.19	1.35	1.84	0.85	1.18	1.35	1.85	0.85	1.18
dimers representing different interaction types	591	0.71	1.14	0.62	0.99	0.71	1.12	0.62	0.98	0.72	1.13
sum of sets 1−6	1048	1.86	3.15	1.30	1.89	1.19	1.77	1.28	1.84	1.23	1.90
all	1639	1.44	2.61	1.06	1.63	1.02	1.56	1.04	1.59	1.05	1.66

S2 in the Supporting Information. For the tentative new sets of vdW parameters in GA optimization, the densities were predicted through interpolation with eq 3. As shown in Table S2 in the Supporting Information, the densities of the two distinct vdW parameter sets are still within small ranges of the experimental values (the mean deviation is 10.5%), which is important to allow the linear interpolation.

GA optimizations were run several times to improve the fitness. The parameters that control GA optimization were set similar to those in our previous work.[6] Although GA optimization was automatic, human intuition was needed to redefine atom types and adjust the searching space to improve the fitting performance. The final optimized vdW set is listed in Table 1.

The assessment of the approach to predict liquid densities by interpolating/extrapolating mean residue−residue interaction energies is presented in Figure 2. It demonstrates the comparisons of the experimental, predicted, and calculated liquid densities from actual MD simulations. The AUE and APE between predicted and experimental are 0.022 g cm^{-3} and 2.34%, respectively (Figure 2a), while the AUE and APE between the predicted and MD densities are 0.015 g cm^{-3} and 1.80%, respectively (Figure 2c). To justify the use of a single NVT snapshot in density prediction, we recalculated the extrapolation/interpolation parameters and predicted the densities using another NVT snapshot (MD Frame #100). As shown in Figure 2e, the predicted densities of the two snapshots are highly correlated: the R^2, AUE, and APE are 1.0, 0.001, and 0.13%, respectively. The negligible APE between the two sets of predicted densities clearly supports our protocol of using one NVT snapshot in density prediction.

This vdW parametrization protocol can be expanded to use multiple vdW parameter sets in interpolation/extrapolation, to apply multiple NVT snapshots for more accurate calculation of mean residue−residue interaction energies, and to deal with other liquid properties (such as heats of vaporization) as well.

3.2. Interaction Energies. The interaction energies of 1639 dimers calculated by *ab initio* and five molecular mechanical models are listed in Table S1 in the Supporting Information. The performance of the five molecular models, namely, FF99/GAFF, TL-FF99vdW, TL-OptvdW, TA-FF99vdW, and TA_OptvdW, are summarized in Table 2. It is obvious that the polarizable models are much better than the additive one: the RMSEs are 2.61, 1.63, 1.56, 1.59, and 1.66 kcal/mol for the above five molecular mechanical models, respectively. Interestingly, all five models achieved similar performance for set 7 which has 590 dimers representing different types of molecular interactions. If only the amino acid analogues and nucleic acid bases are considered (sets 1−6), the polarizable models have an even bigger advantage over the additive one.

Among sets 1−6, the amino acid side chain analogues (set 2) showed the largest difference. As noted in our earlier work, with the FF99vdW set, the AUE reduced from 2.61 in additive FF99 to 1.42 and 1.31 in TL and TA, respectively. The RMSE also reduced from 4.09 in additive FF99 to 1.97 and 1.86 in TL and TA. The optimization of the vdW parameters using the TL model further reduced the AUE to 1.31 and RMSE to 1.79. When the optimized vdW was tested on the TA model, the AUE was retained at a similar level compared to FF99vdW (1.39 vs 1.37), while RMSE increased from 1.86 to 2.02, by 0.16, understandably, because the optimization was performed on the TL model only. Nevertheless, it is clear that the TL and TA models are notably better than the additive model. Notable improvements are seen in nucleic acid base steps, with AUE reduced from 1.35 to 0.85 and RMSE reduced from 1.84 and 1.85 to 1.18 after vdW optimization. Overall, when sets 1−6 are evaluated, the polarizable models show clear advantages.

Among the four polarizable molecular mechanical models, TL-OptvdW has achieved a marginally better performance than the other three models. However, for set 6, the 100 dimers of nucleic acid base steps, the two models utilizing the optimized vdW set notably outperform the two using the FF99vdW set.

An important practice in protein force field development is to investigate how a force field parametrized using small building blocks of amino acids propagates the calculation errors to larger molecules. However, it is impractical to accurately calculate the energies of large peptides with high level *ab initio* approaches. Here we calculated the interaction energies of ACE-GLY-NME dimers studied by Wang et al.[63] using high-level *ab initio* models. The geometries of the four conformations are shown in Figure 3. The interaction energies in the CBS limit were obtained by extrapolating the interaction energies at the MP2/aug-cc-pVDZ, MP2/aug-cc-pVTZ, and MP2/aug-cc-pVQZ levels with and without BSSE correction. We consider this comparison a rather critical test because this is the only realistic high level model of the main chain interactions in proteins. Thus, we intentionally excluded this data set in the fitting. Overall, the performance of FF99vdW and the optimized vdW sets are comparable and all polarizable models are significantly better than the additive model, as indicated in Table 3. It is not surprising that the AUE and RMSE of the FF99/GAFF additive model are more than 2 times larger. Such a large degree of improvement illustrates the superiority of the polarizable models. It is important to note that all the interaction energy calculations including the ACE-

dx.doi.org/10.1021/jp3019759 | J. Phys. Chem. B 2012, 116, 7088−7101

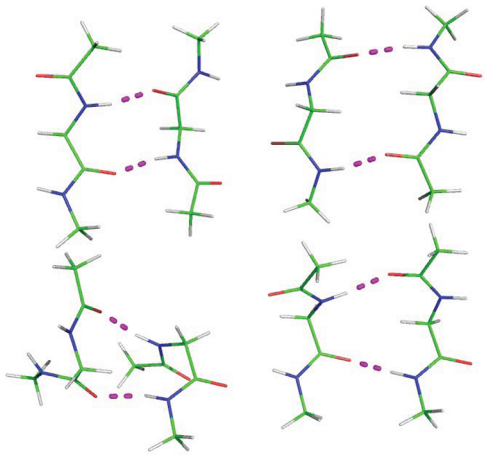

Figure 3. *Ab initio* conformations of ACE-GLY-NME dimer:[63] (1) upper left: abbc5, antiparallel beta C5 conformation; (2) upper right: abbc7, antiparallel beta C7 conformation, (3) lower left: ahh, alpha helical conformation, and (4) lower right: pbb, parallel beta conformation. The hydrogen bonds are shown by dashed lines.

Table 3. Conformational Energies of ACE-GLY-NME Dimer (kcal/mol)

		additive	Thole-linear		Thole-Amoeba	
conf.	*ab initio*[a]	FF99	FF99 vdW	Opt. vdW	FF99 vdW	Opt. vdW
abbc5	−14.98	−13.68	−15.24	−14.94	−15.34	−15.04
abbc7	−21.38	−17.02	−22.81	−22.52	−23.00	−22.70
ahh	−15.89	−17.27	−14.85	−14.18	−14.86	−14.19
pbb	−18.17	−16.13	−19.06	−18.73	−19.22	−18.88
AUE		2.27	0.90	0.86	1.02	0.95
RMSE		2.59	1.07	1.07	1.11	1.13

[a]Extrapolated using the BSSE corrected MP2/aug-cc-pVDZ, MP2/aug-cc-pVTZ, and MP2/aug-cc-pVQZ energies with CCSD(T)/cc-pVDZ correction. The dimer geometries were optimized at the MP2/6-311+G** level of theory (see Wang et al.[63] for detail).

GLY-NME dimers were calculated using the *ab initio* geometries. This is necessary, since the minimized structures depend on both the terms that we intend to test (i.e., nonbonded forces between the peptides) and those that have yet to be refined which would render the QM and MM interaction energies incomparable. Particularly, for ACE-GLY-NME dimers, the torsional angle terms, which will be tuned in the final stage according to our force field development process, have significant impact on the minimized structures.

As the interaction energies were calculated using the *ab initio* geometries without further minimization, it is necessary for us to check if the minimizations significantly distort the *ab initio* optimized geometries. We selected a subset of set 7 for this purpose. All the entries in this subset have equilibrium geometries (fully optimized, not in the dissociation curves). Encouragingly, the minimized geometries using the TL-OptvdW model are very close to *ab initio* ones. The mean and rms of root-mean-square displacements (rmsd) are 0.222 and 0.277 Å, respectively. To investigate if the two monomers come closer or further away after minimizations, we identified the shortest atomic distances between two monomers based on the *ab initio* geometries; then, the distances of the same atom pairs were calculated for the minimized geometries by TL-OptvdW. Comparing the two sets of distances, we found that there is no systematic difference, as the mean difference is close to zero (0.029 Å). The AUE and RMSE of the differences are 0.168 and 0.201 Å, respectively. Moreover, compared to the high-level *ab initio* model, the prediction errors of interaction energies with and without minimization are also very close: the AUE are 0.68 and 0.80 kcal/mol for the *ab initio* and minimized geometries, respectively, and the RMSE are 0.96 and 1.09 kcal/mol for the two sets of geometries, respectively.

3.3. Molecular Property Calculations. Although the van der Waals optimization was performed on the liquid densities and interaction energies only, improvements on other properties are expected, particularly the heats of vaporization, can also be better predicted, because of the improved interactions. We have found that the densities and heats of vaporization were improved almost simultaneously when we adjust the radius and well depth parameters of several classes of compounds in a recent publication.[38]

For the 25 molecule training set, the experimental and calculated densities and heats of vaporization of the training set molecules calculated by five molecular mechanical models are listed in Tables 4 and 5, respectively. The average percent errors of the liquid densities are 3.83, 6.37, 2.70, 6.20, and 2.73% for the FF99/GAFF, TL-FF99vdW, TL-OptvdW, TA-FF99vdW, and TA-OptvdW models, respectively. It is obvious that TL-OptvdW and TA-OptvdW outperform the other molecular mechanical models in density calculations. However, for the heats of vaporization, the best two models are TL-OptvdW and FF99/GAFF, which have achieved an RMSE of 0.98 and 1.11 kcal/mol, respectively.

We note that the two polarizable models that utilize the FF99vdW parameter set have the largest prediction errors in both densities and H_{vap}. This is understandable because the existing vdW parameters, FF99vdW, have been optimized for fixed charge models. Furthermore, the polarizable models include the interactions between the induced dipoles, whereas the physical origin of the R^{-6} dispersion term is the interaction between spontaneous and induced dipoles. Thus, with explicit inclusion of the interactions between the induced dipoles, the models are expected to be more attractive, leading to an overall higher liquid density. This was indeed the case. With FF99vdW, the average densities of the 25 liquids in the TL-FF99vdW and TA-FF99vdW models were, respectively, 0.046 g/cm^3 (5.7%) and 0.043 g/cm^3 (5.4%) higher than the average of experimental densities, whereas the FF99/GAFF fixed charge model was only 0.012 g/cm^3 (1.6%) higher. After the optimization, this systematic error was significantly reduced and the average differences were reduced to 0.001 g/cm^3 (0.13%) and 0.004 g/cm^3 (0.52%) for the TL-OptvdW and TA-OptvdW models, respectively.

In addition to the increased densities, the inclusion of the polarizability also has a significant impact on the heats of vaporization. In the fixed charge FF99/GAFF model, the heats of vaporization was about 0.57 kcal/mol (7.6%) lower than the average experimental value. However, in the polarizable models TL-FF99vdW and TA-FF99vdW, the average heats of vaporization were 0.88 (9.9%) and 1.07 kcal/mol (12.1%) higher than the average experimental value. After the optimization, these large systematic errors were reduced to 0.21 (0.9%) and 0.54 kcal/mol (4.0%) in the TL-OptvdW and TA-OptvdW models, respectively.

Unlike densities and heats of vaporization, the solvation free energies are less affected by the van der Waals parameters. Oostenbrink and van Gunsteren pointed out that it was not

Table 5. Heats of Vaporization of 25 Compounds in the Training Set (kcal/mol)

				additive	Thole-linear		Thole-Amoeba	
no.	compound	expt.	temp. (°C)	GAFF	FF99 vdW	Opt. vdW	FF99 vdW	Opt. vdW
1	isobutane	4.57	25	3.48 ± 0.02	5.28 ± 0.06	4.92 ± 0.05	5.26 ± 0.06	5.00 ± 0.05
2	trans-2-butene	5.15	25	3.08 ± 0.01	4.26 ± 0.00	4.62 ± 0.00	4.26 ± 0.00	4.63 ± 0.01
3	benzene	7.89	25	6.38 ± 0.02	7.44 ± 0.00	6.79 ± 0.00	7.51 ± 0.00	6.84 ± 0.00
4	ethanol	10.04	25	10.15 ± 0.01	12.58 ± 0.02	12.71 ± 0.03	13.65 ± 0.02	14.55 ± 0.02
5	acetic acid	12.33	25	13.38 ± 0.02	13.39 ± 0.10	12.68 ± 0.04		13.63 ± 0.03
6	methylamine	5.59	25	7.47 ± 0.01	7.97 ± 0.01	5.54 ± 0.08	8.14 ± 0.00	5.63 ± 0.01
7	*N*-methyl acetamide	13.30	100	12.57 ± 0.02	16.73 ± 0.03	15.70 ± 0.03	16.74 ± 0.00	15.90 ± 0.03
8	methanol	8.84	25	9.72 ± 0.01	9.49 ± 0.00	9.60 ± 0.00	10.25 ± 0.01	10.96 ± 0.01
9	phenol	13.82	25	11.98 ± 0.03	13.92 ± 0.02	13.77 ± 0.01	13.56 ± 0.03	14.63 ± 0.01
10	ethanethiol	6.52	25	4.95 ± 0.01	5.66 ± 0.00	5.48 ± 0.00	5.69 ± 0.00	5.64 ± 0.01
11	dimethyl ether	5.14	−24.6	4.64 ± 0.01	5.63 ± 0.00	5.07 ± 0.01	5.62 ± 0.00	5.06 ± 0.00
12	dimethyl sulfide	6.61	25	4.44 ± 0.01	5.73 ± 0.01	5.56 ± 0.01	5.82 ± 0.01	5.64 ± 0.01
13	acetone	7.47	25	7.20 ± 0.02	8.53 ± 0.04	7.88 ± 0.04	8.54 ± 0.04	7.99 ± 0.04
14	dimethyl amine	6.08	25	6.37 ± 0.01	6.84 ± 0.00	6.43 ± 0.01	6.93 ± 0.00	5.65 ± 0.01
15	trimethylamine	5.18	25	4.60 ± 0.02	6.90 ± 0.04	4.41 ± 0.04	6.86 ± 0.04	4.38 ± 0.04
16	aniline	12.91	25	12.16 ± 0.02	13.87 ± 0.01	12.85 ± 0.02	13.88 ± 0.01	13.03 ± 0.01
17	acetonitrile	7.87	25	7.19 ± 0.01	10.00 ± 0.02	9.13 ± 0.01	10.06 ± 0.02	9.20 ± 0.01
18	*N*,*N*-dimethyl acetamide	11.75	25	11.13 ± 0.01	14.34 ± 0.01	13.14 ± 0.01	14.34 ± 0.01	13.10 ± 0.01
19	dimethyl sulfoxide	10.30	189	8.84 ± 0.02	10.34 ± 0.04	9.91 ± 0.04	12.71 ± 0.04	12.42 ± 0.04
20	trichloromethane	7.48	25	6.84 ± 0.01	7.28 ± 0.00	6.77 ± 0.00	7.26 ± 0.00	6.76 ± 0.00
21	tetrachloromethane	7.75	25	8.02 ± 0.01	8.12 ± 0.00	7.59 ± 0.00	8.17 ± 0.00	7.66 ± 0.00
22	bromomethane	5.45	25	4.95 ± 0.01	5.08 ± 2.00	4.88 ± 0.00	5.13 ± 0.00	4.93 ± 0.00
23	tetrahydrofuran	7.65	25	7.59 ± 0.02	9.65 ± 0.00	8.44 ± 0.00	9.64 ± 0.00	8.59 ± 0.00
24	pyridine	9.56	25	8.81 ± 0.03	10.94 ± 0.12	9.99 ± 0.13	11.12 ± 0.12	10.13 ± 0.12
25	quinoline	14.18	25	13.18 ± 0.02	15.56 ± 0.11	14.78 ± 0.10	15.72 ± 0.08	14.98 ± 0.10
	average difference		−0.572	0.884	0.208		1.073	0.540
	average percent difference		−7.57%	9.93%	0.88%		12.10%	3.99%
	AUE		0.93	1.18	0.73		1.38	1.02
	RMSE		1.11	1.47	0.98		1.69	1.40

Table 6. Experimental and Calculated Hydration Energies (kcal/mol)

			Additive	Thole-linear		Thole-Amoeba	
no.	compound	expt.[a]	GAFF	FF99 vdW	Opt. vdW	FF99 vdW	Opt. vdW
1	isobutane	2.22	2.25 ± 0.01	1.78 ± 0.03	1.99 ± 0.02	1.82 ± 0.03	2.12 ± 0.02
2	benzene	−0.86	−0.75 ± 0.07	−2.09 ± 0.11	−1.90 ± 0.11	−2.11 ± 0.07	−1.77 ± 0.09
3	ethanol	−5.00	−4.34 ± 0.07	−5.78 ± 0.11	−7.57 ± 0.14	−6.45 ± 0.12	−9.04 ± 0.14
4	acetic acid	−6.70	−6.02 ± 0.12	−1.76 ± 0.16	−4.30 ± 0.16	−1.23 ± 0.26	−5.74 ± 0.21
5	methylamine	−4.60	−4.74 ± 0.06	−5.27 ± 0.12	−7.57 ± 0.21	−5.48 ± 0.13	−6.90 ± 0.12
6	*N*-methylaceticamide	−10.00	−7.81 ± 0.09	−11.13 ± 0.14	−10.62 ± 0.17	−10.98 ± 0.12	−10.59 ± 0.16
7	phenol	−6.61	−4.59 ± 0.07	−6.31 ± 0.16	−6.53 ± 0.15	−6.50 ± 0.20	−8.05 ± 0.18
8	ethanethiol	−1.30	−0.41 ± 0.03	−1.25 ± 0.09	−1.30 ± 0.09	−1.75 ± 0.07	−1.58 ± 0.09
9	dimethyl ether	−1.91	−0.47 ± 0.05	−1.25 ± 0.06	−0.82 ± 0.08	−1.28 ± 0.07	−0.87 ± 0.06
10	acetone	−3.80	−3.52 ± 0.05	−4.88 ± 0.10	−4.35 ± 0.08	−4.72 ± 0.09	−4.59 ± 0.09
11	dimethylamine	−4.28	−2.54 ± 0.07	−2.91 ± 0.10	−3.64 ± 0.15	−2.94 ± 0.09	−2.83 ± 0.12
12	trimethylamine	−3.23	−0.32 ± 0.04	−2.39 ± 0.10	−2.16 ± 0.09	−2.56 ± 0.12	−1.99 ± 0.12
13	dimethyl sulfoxide	−8.71	−8.58 ± 0.11	−9.46 ± 0.12	−9.73 ± 0.15	−9.95 ± 0.15	−10.01 ± 0.12
14	bromomethane	−0.82	−0.08 ± 0.02	−0.27 ± 0.03	−0.11 ± 0.04	−0.18 ± 0.04	−0.12 ± 0.03
15	pyridine	−4.69	−3.08 ± 0.05	−6.34 ± 0.09	−5.72 ± 0.13	−6.46 ± 0.08	−6.17 ± 0.11
	average difference		1.019	0.065	−0.269	−0.032	−0.523
	average percent difference		−32.82%	−0.33%	3.47%	3.31%	8.15%
	AUE		1.04	1.10	1.07	1.21	1.24
	RMSE		1.35	1.56	1.38	1.72	1.54

[a]Nos. 2, 3, 7, 9, and 13 come from ref 46, and the others, from ref 45.

possible to obtain a set of charges for the polar groups that could simultaneously reproduce the thermodynamic properties of a range of pure liquids and the hydration enthalpy with high accuracy.[64] Indeed, the performance of the five molecular mechanical models is very similar in calculating the hydration energies of 15 compounds with thermodynamic integration. Encouragingly, the optimized vdW parameter set still outperforms the FF99 vdW parameter set in conjunction with both

dx.doi.org/10.1021/jp3019759 | J. Phys. Chem. B 2012, 116, 7088−7101

Table 7. Densities of 35 Compounds in the Test Set (g/cm^3)

				additive	Thole-linear		Thole-Ameoba	
no.	compound	expt.[a]	temp. (°C)	GAFF	FF99 vdW	Opt. vdW	FF99 vdW	Opt. vdW
1	1-butyne	0.678	0	0.738 ± 0.000	0.748 ± 0.000	0.711 ± 0.000	0.748 ± 0.000	0.711 ± 0.000
2	fluorobenzene	1.023	20	0.989 ± 0.001	1.005 ± 0.000	0.989 ± 0.001	1.005 ± 0.000	0.989 ± 0.001
3	propanol	0.800	25	0.811 ± 0.001	0.821 ± 0.000	0.764 ± 0.001	0.828 ± 0.000	0.770 ± 0.001
4	propanethiol	0.836	25	0.833 ± 0.000	0.835 ± 0.000	0.820 ± 0.000	0.836 ± 0.000	0.820 ± 0.000
5	ethyl methyl ether	0.721	7.35	0.728 ± 0.000	0.741 ± 0.000	0.708 ± 0.000	0.740 ± 0.000	0.708 ± 0.000
6	ethyl methyl sulfide	0.837	25	0.801 ± 0.000	0.818 ± 0.000	0.801 ± 0.000	0.817 ± 0.000	0.802 ± 0.000
7	dimethyl disulfide	1.057	25	1.019 ± 0.000	1.027 ± 0.000	1.025 ± 0.000	1.028 ± 0.001	1.024 ± 0.001
8	acetaldehyde	0.783	18	0.786 ± 0.000	0.800 ± 0.001	0.739 ± 0.000	0.800 ± 0.000	0.740 ± 0.000
9	butanone	0.800	25	0.784 ± 0.000	0.802 ± 0.000	0.778 ± 0.000	0.802 ± 0.000	0.778 ± 0.001
10	propanoic acid	0.988	25	1.025 ± 0.001	1.032 ± 0.001	0.939 ± 0.000	1.034 ± 0.001	0.944 ± 0.000
11	*N*-methylpropanamide	0.931	25	0.931 ± 0.000	0.963 ± 0.000	0.929 ± 0.001	0.961 ± 0.001	0.929 ± 0.001
12	methylacetate	0.928	25	0.970 ± 0.001	0.989 ± 0.000	0.954 ± 0.001	0.989 ± 0.001	0.953 ± 0.000
13	methyl benzoate	1.089	20	1.107 ± 0.000	1.115 ± 0.001	1.090 ± 0.000	1.112 ± 0.001	1.089 ± 0.000
14	nitromethane	1.140	25	1.232 ± 0.000	1.244 ± 0.000	1.205 ± 0.001	1.245 ± 0.000	1.205 ± 0.001
15	benzonitrile	1.001	25	1.028 ± 0.000	1.040 ± 0.000	1.011 ± 0.000	1.040 ± 0.000	1.012 ± 0.000
16	furan	0.951	20	0.974 ± 0.000	0.983 ± 0.001	0.951 ± 0.000	0.982 ± 0.000	0.952 ± 0.000
17	pyridazine	1.103	25	1.088 ± 0.000	1.131 ± 0.000	1.092 ± 0.001	1.132 ± 0.001	1.092 ± 0.000
18	pyrrole	0.966	25	1.015 ± 0.000	1.037 ± 0.001	1.003 ± 0.000	1.042 ± 0.001	1.006 ± 0.000
19	oxazole	1.080	25	1.145 ± 0.000	1.164 ± 0.001	1.125 ± 0.001	1.163 ± 0.001	1.124 ± 0.000
20	toluene	0.8668	20	0.855 ± 0.001	0.869 ± 0.001	0.854 ± 0.000	0.868 ± 0.001	0.853 ± 0.000
21	ethylbenzene	0.8626	25	0.844 ± 0.000	0.854 ± 0.000	0.837 ± 0.000	0.853 ± 0.001	0.836 ± 0.000
22	2-methyl-1-butene	0.6623	20	0.622 ± 0.000	0.634 ± 0.001	0.640 ± 0.000	0.632 ± 0.001	0.639 ± 0.000
23	butanoic acid	0.9528	25	0.995 ± 0.001	1.053 ± 0.001	1.023 ± 0.001	-	1.026 ± 0.000
24	2,3-dimethylbutane	0.6616	20	0.662 ± 0.000	0.662 ± 0.000	0.646 ± 0.000	0.662 ± 0.000	0.646 ± 0.000
25	cyclohexene	0.811	20	0.779 ± 0.001	0.784 ± 0.000	0.776 ± 0.000	0.782 ± 0.000	0.775 ± 0.000
26	tripropylamine	0.7558	20	0.768 ± 0.001	0.775 ± 0.000	0.736 ± 0.000	0.777 ± 0.000	0.734 ± 0.001
27	propylamine	0.711	25	0.776 ± 0.000	0.813 ± 0.000	0.727 ± 0.001	0.820 ± 0.000	0.756 ± 0.001
28	diethylamine	0.699	25	0.742 ± 0.000	0.749 ± 0.001	0.656 ± 0.000	0.749 ± 0.000	0.657 ± 0.000
29	triethylamine	0.723	25	0.751 ± 0.001	0.751 ± 0.000	0.693 ± 0.000	0.750 ± 0.000	0.689 ± 0.000
30	aziridine	0.831	25	0.835 ± 0.000	0.888 ± 0.001	0.805 ± 0.001	0.893 ± 0.000	0.812 ± 0.001
31	azetidine	0.841	25	0.827 ± 0.000	0.873 ± 0.001	0.826 ± 0.001	0.879 ± 0.000	0.833 ± 0.000
32	pyrrolidine	0.854	25	0.888 ± 0.000	0.902 ± 0.001	0.813 ± 0.001	0.902 ± 0.000	0.817 ± 0.001
33	piperidine	0.857	25	0.891 ± 0.001	0.908 ± 0.000	0.842 ± 0.000	0.910 ± 0.001	0.844 ± 0.001
34	dimethyl hydrogen phosphate	1.3225	20	1.427 ± 0.001	1.448 ± 0.000	1.369 ± 0.000	1.448 ± 0.000	1.383 ± 0.001
	APE	3.46%		4.56%	3.17%	4.50		3.26%
	AUE	0.031		0.041	0.028	0.040		0.029
	RMSE	0.040		0.052	0.032	0.051		0.034

[a]The following is the source of experimental data other than ref 38: nos. 13−16, ref 42; no. 18, ref 39; nos. 19 and 20, ref 41; nos. 21−27 and 35, ref 43; nos. 28−34, ref 40.

the Thole linear and Amoeba-like polarizable models, and the RMSE of the four polarizable molecular mechanical models are 1.56, 1.38, 1.72, and 1.54 kcal/mol for TL-FF99vdW, TL-OptvdW, TA-FF99vdW, and TA-OptvdW, respectively. The experimental and calculated hydration free energies of 15 compounds are summarized in Table 6. The individual terms of TI calculations as well as their uncertainties are listed in Table S3 in the Supporting Information.

There are 34 molecules in the test set. The experimental and calculated densities and heats of vaporization of the test molecules by three molecular mechanical models are listed in Tables 7 and 8. As expected, the TL-OptvdW and TA-OptvdW models achieved a significantly better performance than the other three molecular mechanical models in both density and H_{vap} calculations: for density calculations, the APE are 3.46, 4.56, 3.17, 4.50, and 3.26% for FF99/GAFF, TL-FF99vdW, TL-OptvdW, TA-FF99vdW, and TA_OptvdW, respectively; for H_{vap}, the RMSE are 1.80, 2.48, 1.62, 2.10, and 1.62 kcal/mol for the five aforementioned models accordingly. Compared to the training set, the RMSE of H_{vap} for the test set are much larger. Even through, it is unreasonable to reach a conclusion that our new van der Waals parameter set is overfit, as the RMSE of all five molecular mechanical models including FF99/GAFF, TL-FF99vdW, and TA-FF99vdW are proportionally increased for the test set.

The overall performance of the five molecular mechanical models is demonstrated in the 2D-column plot of Figure 4. It is shown that the two polarizable models utilizing the optimized van der Waals parameter set outperform the additive model and the two polarizable models utilizing the FF99 van der Waals parameter set. The advantage of polarizable models over the additive one becomes obvious when analyzing the results of the interaction energy calculations. The overall rank of the five molecular mechanical models in condensed property calculations is TL-OptvdW > TA-OptvdW ∼ FF99/GAFF > TL-FF99vdW > TA-FF99vdW. In conclusion, the optimized van der Waals parameter set has been successfully developed, and it achieves a dramatically better performance than the FF99 vdW

dx.doi.org/10.1021/jp3019759 | J. Phys. Chem. B 2012, 116, 7088−7101

Table 8. Heats of Vaporization for 34 Compounds in the Test Set

				additive	Thole-linear		Thole-Amoeba	
no.	compound	temp. (°C)	expt.[a]	GAFF	FF99 vdW	Opt. vdW	FF99 vdW	Opt. vdW
1	1-butyne	25	5.58	6.58 ± 0.00	8.67 ± 0.01	7.52 ± 0.00	9.02 ± 0.00	7.93 ± 0.00
2	fluorobenzene	25	8.29	5.85 ± 0.01	7.86 ± 0.02	7.56 ± 0.03	7.93 ± 0.02	7.60 ± 0.02
3	propanol	25	11.35	11.65 ± 0.00	12.32 ± 0.01	12.08 ± 0.01	13.04 ± 0.00	13.44 ± 0.01
4	propanethiol	25	7.62	5.01 ± 0.00	6.41 ± 0.01	6.09 ± 0.00	6.43 ± 0.01	6.24 ± 0.00
5	ethyl methyl ether	7.35	5.91	4.17 ± 0.00	6.03 ± 0.01	5.37 ± 0.00	6.02 ± 0.01	5.42 ± 0.01
6	ethyl methyl sulfide	25	7.61	4.50 ± 0.01	6.44 ± 0.00	6.13 ± 0.00	6.45 ± 0.00	6.24 ± 0.00
7	dimethyl disulfide	25	9.06	5.69 ± 0.01	7.33 ± 0.00	7.28 ± 0.01	7.33 ± 0.01	7.33 ± 0.01
8	acetaldehyde	25	6.24	5.21 ± 0.01	6.90 ± 0.01	5.90 ± 0.01	6.99 ± 0.01	6.04 ± 0.01
9	butanone	25	8.35	6.96 ± 0.01	9.23 ± 0.02	8.42 ± 0.01	9.21 ± 0.01	8.60 ± 0.01
10	propanoic acid	25	13.15	14.09 ± 0.01	13.77 ± 0.02	11.89 ± 0.03	14.81 ± 0.03	13.16 ± 0.01
11	*N*-methylpropanamide	25	15.5	13.64 ± 0.00	18.81 ± 0.01	17.53 ± 0.02	18.80 ± 0.02	17.78 ± 0.01
12	methylacetate	25	7.72	7.86 ± 0.03	9.89 ± 0.03	8.93 ± 0.04	9.90 ± 0.04	9.01 ± 0.03
13	methyl benzoate	25	13.28	12.79 ± 0.01	14.85 ± 0.01	13.64 ± 0.03	14.84 ± 0.02	13.62 ± 0.01
14	nitromethane	25	9.17	11.51 ± 0.02	12.15 ± 0.03	10.91 ± 0.03	12.20 ± 0.03	11.14 ± 0.03
15	benzonitrile	25	12.54	12.48 ± 0.02	14.28 ± 0.01	13.19 ± 0.00	14.27 ± 0.01	13.10 ± 0.00
16	furan	25	6.62	5.26 ± 0.00	7.05 ± 0.00	6.49 ± 0.00	7.12 ± 0.00	6.48 ± 0.00
17	pyridazine	25	12.78	11.20 ± 0.01	14.55 ± 0.01	13.26 ± 0.01	14.60 ± 0.00	13.19 ± 0.01
18	pyrrole	25	10.84	10.39 ± 0.00	16.26 ± 0.01	15.53 ± 0.00	16.39 ± 0.01	15.58 ± 0.00
19	oxazole	25	7.77	8.01 ± 0.01	10.01 ± 0.01	9.13 ± 0.00	10.01 ± 0.01	9.07 ± 0.00
20	toluene	25	8.84	6.92 ± 0.01	8.99 ± 0.02	8.59 ± 0.02	9.09 ± 0.02	8.69 ± 0.02
21	ethylbenzene	25	10.1	7.59 ± 0.01	9.64 ± 0.01	9.09 ± 0.01	9.61 ± 0.01	9.13 ± 0.00
22	2-methyl-1-butene	25	6.26	3.51 ± 0.01	5.71 ± 0.02	5.93 ± 0.02	5.79 ± 0.03	6.09 ± 0.02
23	butanoic acid	25	13.86	14.37 ± 0.03	15.10 ± 0.25	16.09 ± 0.03	-	17.70 ± 0.03
24	2,3-dimethylbutane	25	7.01	5.25 ± 0.00	7.09 ± 0.01	6.55 ± 0.01	7.17 ± 0.01	6.62 ± 0.00
25	cyclohexene	25	8.02	5.78 ± 0.01	7.66 ± 0.00	7.42 ± 0.00	7.72 ± 0.00	7.59 ± 0.00
26	tripropylamine	25	11.03	9.93 ± 0.02	12.48 ± 0.01	9.76 ± 0.02	12.57 ± 0.02	9.74 ± 0.01
27	propylamine	25	7.47	8.91 ± 0.00	14.33 ± 0.02	10.50 ± 0.02	12.79 ± 0.01	10.20 ± 0.02
28	diethylamine	25	7.48	6.79 ± 0.03	11.42 ± 0.05	8.78 ± 0.04	8.21 ± 0.03	5.91 ± 0.03
29	triethylamine	25	8.33	7.33 ± 0.02	13.86 ± 0.01	11.68 ± 0.01	9.05 ± 0.01	6.59 ± 0.00
30	aziridine	25	8.09	7.06 ± 0.01	10.94 ± 0.01	9.61 ± 0.00	9.90 ± 0.01	8.48 ± 0.01
31	azetidine	25	8.17	7.11 ± 0.02	11.24 ± 0.04	9.11 ± 0.03	9.54 ± 0.03	9.41 ± 0.02
32	pyrrolidine	25	8.95	6.58 ± 0.00	8.67 ± 0.01	7.52 ± 0.00	10.70 ± 0.00	7.99 ± 0.02
33	piperidine	25	9.39	5.85 ± 0.01	7.86 ± 0.02	7.56 ± 0.03	11.83 ± 0.03	9.28 ± 0.02
	AUE	1.53		1.84	1.29	1.63		1.20
	RMSE	1.80		2.48	1.62	2.10		1.62

[a]The following is the source of experimental data other than ref 38: nos. 13, 14, and 16, ref 42; no. 20, ref 41; nos. 21–27, ref 44; nos. 28–34, ref 40. Energies are in kcal/mol.

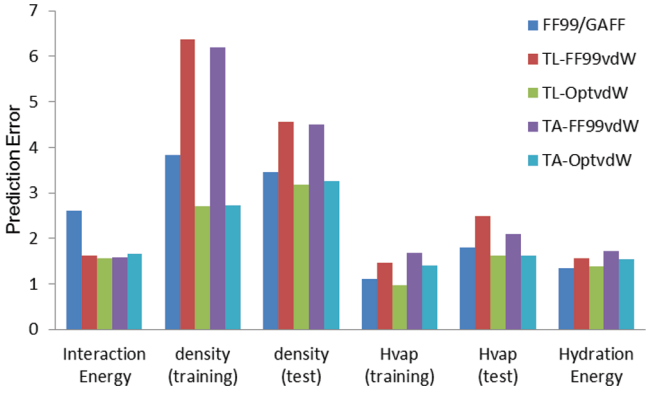

Figure 4. Performance of the five molecular mechanical models: for density, the prediction error is measured as APE (average percent error), for interaction energy, heat of vaporization and hydration energy, and the prediction errors are measured by RMSE (root-mean-square error).

parameter set in calculating three condensed-phase properties of a large set of compounds.

It is encouraging that TA-OptvdW has also achieved a satisfactory performance in both interaction energy and bulk molecular property calculations. We further investigated how well the optimized vdW set are transferable among different polarizable models in interaction energy calculations. The results are summarized in Table 9. Encouragingly, the transferability between the Thole linear and Amoeba-like polarizable models is very good as long as the screen factor is not far away from the optimized values (the screening factor is equal to 2.587 for the Thole linear and 1.621 for Thole Amoeba-like models). As for the bulk property calculations, in most cases, the predicted densities, H_{vap}, or solvation free energies obtained by TL-OptvdW and TA-OptvdW are comparable to each other (Tables 4–8). However, a difference may occur for some molecules that form strong hydrogen bonds in pure solvent or aqueous solution, such as acids and amines. The reason that leads to this difference is that the screening effect of the Thole linear model is stronger than that of the Thole Amoeba-like model when the separation distance

dx.doi.org/10.1021/jp3019759 | J. Phys. Chem. B 2012, 116, 7088–7101

Table 9. Transferability of the Optimized van der Waals Parameters among Different Polarizable Models in Interaction Energy Calculation[a]

polarizable model	screening factor κ	AUE	RMSE
Thole-Linear Charges and Atomic Polarizabilities			
Applequist		1.229	2.953
linear	2.587	1.015	1.562
linear	2.441	1.036	1.619
linear	1.662	1.202	2.558
Amoeba	1.621	1.049	1.658
Amoeba	1.369	1.125	1.957
Amoeba	1.330	1.136	2.018
Amoeba	1.205	1.171	2.244
Thole-Amoeba Charges and Atomic Polarizabilities			
Applequist		1.229	2.951
linear	2.587	1.014	1.563
linear	2.441	1.036	1.621
linear	1.662	1.203	2.563
Amoeba	1.621	1.048	1.660
Amoeba	1.369	1.125	1.960
Amoeba	1.330	1.136	2.021
Amoeba	1.205	1.170	2.247

[a]The performance of each model is evaluated by AUE (average unsigned errors) and RMSE (root-mean-square error) for 1639 dimers listed in Table S1 in the Supporting Information.

between two atoms is smaller than 2.5 Å. The screening effect as a function of separation distance for both models is shown in Figure S1 in the Supporting Information. It is expected that the performance of the Thole Amoeba-like model can be further improved after we fine-tune the van der Waals parameters that are involved in hydrogen bonding.

In principle, the approach used in this work can be applied to develop other parameters. For example, Jorgensen et al.[65] developed the OPLS force field by optimizing the parameters, including atomic partial charges, against liquid properties. In AMBER, the partial charges are obtained by fitting the quantum mechanical electrostatic potentials. In which case, adjustment of charges is not recommended. Thus, our adjustments are limited to the van der Waals parameters that are considered more transferable than the partial charges. Nevertheless, a considerably larger data set would be needed if one desires to refine both van der Waals and partial charges.

To improve the quality of our van der Waals parameters further, we plan to introduce more high quality *ab initio* interaction energy data and experimental density and heat of vaporization data to our training and test sets, and to design better atom type definition schemes to reduce the prediction errors. We will also explore if other molecular mechanical properties have a better relationship to liquid density than residue−residue interaction energy.

4. CONCLUSIONS

It is clear that the two nonbonded terms, electrostatic and van der Waals, are tightly coupled. The large average percent error of the FF99 vdW set in density calculation strongly suggests that the reparameterization of vdW parameters for the Thole polarizable models is necessary. Owing to the success of density prediction using mean residue−residue energies, we were able to overcome the challenge of calculating densities through molecular simulations and optimize a large set of vdW parameters efficiently using a genetic algorithm.

The optimized vdW parameter set in conjunction with Thole polarization models performs encouragingly better than the FF99vdW parameter set that is coupled with the additive model.

We believe that this vdW parameter set in combination with both the Thole linear and Thole Amoeba-like polarizable models paves a road to parametrization of the bonded terms and enables us to develop a reliable and accurate molecular mechanical model for studying the structures, energies, and functions of biomolecules.

■ ASSOCIATED CONTENT

Supporting Information

The functional forms of Thole linear (TL) and Thole Amoeba (TA) models are provided in the supporting text. The interaction energies calculated by high-level *ab initio* models as well as the three molecular mechanical models are listed in Table S1. The individual energetic terms in hydration energy calculation using thermodynamic integration are listed in Table S2. The mean inter-residue energy parameters used in density prediction are listed in Table S3. This material is available free of charge via the Internet at http://pubs.acs.org.

■ AUTHOR INFORMATION

Corresponding Author

*E-mail: duan@ucdavis.edu. Fax: (530)-754-9658. Tel: (530)-754-5625.

Notes

The authors declare no competing financial interest.

■ ACKNOWLEDGMENTS

We are grateful to acknowledge the research support from NIH (R01GM79383, Y.D., P.I. and R21GM097617, J.W., P.I.) and the TeraGrid for the computational time (TG-CHE090098, J.W., P.I. and TG-CHE090135, P.C., P.I.).

■ ABBREVIATIONS

vdW: van der Waals
TL: Thole linear polarizable model
TA: Thole Amoeba-like polarizable model
GAFF: general AMBER force field
TL-FF99vdW: Thole linear polarizable model with FF99 van der Waals parameters
TL-OptvdW: Thole linear polarizable model with optimized van der Waals parameters
TA-FF99vdW: Thole Amoeba-like polarizable model with FF99 van der Waals parameters
TA-OptvdW: Thole Amoeba-like polarizable model with optimized van der Waals parameters
AUE: average unsigned errors
RMSE: root-mean-square errors
APE: average percent errors
R^2: correlation coefficient square
H_{vap}: heats of vaporization

■ REFERENCES

(1) Kaminski, G. A.; Stern, H. A.; Berne, B. J.; Friesner, R. A. *J. Phys. Chem. A* **2004**, *108*, 621.
(2) Ponder, J. W.; Case, D. A. *Adv. Protein Chem.* **2003**, *66*, 27.
(3) Ren, P. Y.; Ponder, J. W. *J. Comput. Chem.* **2002**, *23*, 1497.
(4) Cieplak, P.; Caldwell, J.; Kollman, P. A. *J. Comput. Chem.* **2001**, *22*, 1048.

(5) Wang, Z.-X.; Zhang, W.; Wu, C.; Lei, H.; Cieplak, P.; Duan, Y. *J. Comput. Chem.* **2006**, *27*, 781.
(6) Wang, J. M.; Cieplak, P.; Li, J.; Hou, T. J.; Luo, R.; Duan, Y. *J. Phys. Chem. B* **2011**, *115*, 3091.
(7) Wang, J. M.; Cieplak, P.; Li, J.; Wang, J.; Cai, Q.; Hsieh, M. J.; Lei, H. X.; Luo, R.; Duan, Y. *J. Phys. Chem. B* **2011**, *115*, 3100.
(8) Wang, J.; Cieplak, P.; Cai, Q.; Hsieh, M.-J.; Wang, J.; Duan, Y.; Luo, R. *J. Phys. Chem. B* **2012**, in revision.
(9) Brooks, B. R.; Bruccoleri, R. E.; Olafson, B. D.; States, D., J; Swaminathan, S.; Karplus, M. *J. Comput. Chem.* **1983**, *4*, 187.
(10) Jorgensen, W. L.; Maxwell, D. S.; TiradoRives, J. *J. Am. Chem. Soc.* **1996**, *118*, 11225.
(11) Cornell, W. D.; Cieplak, P.; Bayly, C. I.; Gould, I. R.; Merz, K. M.; Ferguson, D. M.; Spellmeyer, D. C.; Fox, T.; Caldwell, J. W.; Kollman, P. A. *J. Am. Chem. Soc.* **1995**, *117*, 5179.
(12) Wang, J.; Cieplak, P.; Kollman, P. A. *J. Comput. Chem.* **2000**, *21*, 1049.
(13) Duan, Y.; Wu, C.; Chowdhury, S.; Lee, M. C.; Xiong, G.; Zhang, W.; Yang, R.; Cieplak, P.; Luo, R.; Lee, T.; Caldwell, J. W.; Wang, J.; Kollman, P. A. *J. Comput. Chem.* **2003**, *24*, 1999.
(14) Wang, J.; Wolf, R. M.; Caldwell, J. W.; Kollman, P. A.; Case, D. A. *J. Comput. Chem.* **2004**, *25*, 1157.
(15) Wang, J. M.; Cieplak, P.; Kollman, P. A. *J. Comput. Chem.* **2000**, *21*, 1049.
(16) Oostenbrink, C.; Soares, T. A.; van der Vegt, N. F.; van Gunsteren, W. F. *Eur. Biophys. J.* **2005**, *34*, 273.
(17) Rappe, A. K.; Casewit, C. J.; Colwell, K. S.; Goddard, W. A.; Skiff, W. M. *J. Am. Chem. Soc.* **1992**, *114*, 10024.
(18) Sun, H. *J. Phys. Chem. B* **1998**, *102*, 7338.
(19) Shi, S. H.; Yan, L.; Yang, Y.; Fisher-Shaulsky, J.; Thacher, T. *J. Comput. Chem.* **2003**, *24*, 1059.
(20) Halgren, T. A. *J. Comput. Chem.* **1996**, *17*, 520.
(21) Kaminski, G. A.; Friesner, R. A.; Tirado-Rives, J.; Jorgensen, W. L. *J. Phys. Chem. B* **2001**, *105*, 6474.
(22) Tsuzuki, S.; Uchimaru, T.; Tanabe, K.; Kuwajima, S. *J. Phys. Chem.* **1994**, *98*, 1830.
(23) Yin, D. X.; Mackerell, A. D. *J. Comput. Chem.* **1998**, *19*, 334.
(24) Chen, I. J.; Yin, D. X.; MacKerell, A. D. *J. Comput. Chem.* **2002**, *23*, 199.
(25) Feller, S. E.; MacKerell, A. D. *J. Phys. Chem. B* **2000**, *104*, 7510.
(26) Wang, J.; Kollman, P. A. *J. Comput. Chem.* **2001**, *22*, 1219.
(27) Wang, J. M.; Krudy, G.; Xie, X. Q.; Wu, C. D.; Holland, G. *J. Chem. Inf. Model.* **2006**, *46*, 2674.
(28) Hou, T. J.; Wang, J. M.; Chen, L. R.; Xu, X. J. *Protein Eng.* **1999**, *12*, 639.
(29) Simon, S.; Duran, M.; Dannenberg, J. J. *J. Chem. Phys.* **1996**, *105*, 11024.
(30) Boys, S. F.; Bernardi, F. *Mol. Phys.* **1970**, *19*, 553.
(31) Truhlar, D. G. *Chem. Phys. Lett.* **1998**, *294*, 45.
(32) Fast, P. L.; Sanchez, M. L.; Truhlar, D. G. *J. Chem. Phys.* **1999**, *111*, 2921.
(33) Sponer, J.; Jurecka, P.; Hobza, P. *J. Am. Chem. Soc.* **2004**, *126*, 10142.
(34) Morgado, C. A.; Jurecka, P.; Svozil, D.; Hobza, P.; Sponer, J. *Phys. Chem. Chem. Phys.* **2010**, *12*, 3522.
(35) Morgado, C. A.; Jurecka, P.; Svozil, D.; Hobza, P.; Sponer, J. *J. Chem. Theory Comput.* **2009**, *5*, 1524.
(36) Svozil, D.; Hobza, P.; Sponer, J. *J. Phys. Chem. B* **2010**, *114*, 1191.
(37) Rezac, J.; Riley, K. E.; Hobza, P. *J. Chem. Theory Comput.* **2011**, *7*, 2427.
(38) Wang, J. M.; Hou, T. J. *J. Chem. Theory Comput.* **2011**, *7*, 2151.
(39) Jorgensen, W. L.; McDonald, N. A. *J. Mol. Struct.: THEOCHEM* **1998**, *424*, 145.
(40) Rizzo, R. C.; Jorgensen, W. L. *J. Am. Chem. Soc.* **1999**, *121*, 4827.
(41) McDonald, N. A.; Jorgensen, W. L. *J. Phys. Chem. B* **1998**, *102*, 8049.
(42) Price, M. L. P.; Ostrovsky, D.; Jorgensen, W. L. *J. Comput. Chem.* **2001**, *22*, 1340.
(43) Lide, D. R. E.*CRC Handbook of Chemistry and Physics,* 86th ed.; CRC Press: Boca Raton, FL, 2005; p 4.
(44) Majer, V.; Svoboda, V.*Enthalpies of Vaporization of Organic Compounds: A Critical Review and Data Compilation* ; Blackwell Scientific Publications: Oxford, U.K., 1985; p 300.
(45) Wang, J. M.; Wang, W.; Huo, S. H.; Lee, M.; Kollman, P. A. *J. Phys. Chem. B* **2001**, *105*, 5055.
(46) Mobley, D. L.; Bayly, C. I.; Cooper, M. D.; Shirts, M. R.; Dill, K. A. *J. Chem. Theory Comput.* **2009**, *5*, 350.
(47) Bayly, C. I.; Cieplak, P.; Cornell, W. D.; Kollman, P. A. *J. Phys. Chem.* **1993**, *97*, 10269.
(48) Cieplak, P.; Dupradeau, F. Y.; Duan, Y.; Wang, J. M. *J. Phys.: Condens. Matter* **2009**, *21*, 333102.
(49) Frisch, M. J.; Trucks, G. W.; Schlegel, H. B.; Scuseria, G. E.; Robb, M. A.; Cheeseman, J. R.; Montgomery, J. A., Jr.; Vreven, T.; Kudin, K. N.; Burant, J. C.; Millam, J. M.; Iyengar, S. S.; Tomasi, J.; Barone, V.; Mennucci, B.; Cossi, M.; Scalmani, G.; Rega, N.; Petersson, G. A.; Nakatsuji, H.; Hada, M.; Ehara, M.; Toyota, K.; Fukuda, R.; Hasegawa, J.; Ishida, M.; Nakajima, T.; Honda, Y.; Kitao, O.; Nakai, H.; Klene, M.; Li, X.; Knox, J. E.; Hratchian, H. P.; Cross, J. B.; Bakken, V.; Adamo, C.; Jaramillo, J.; Gomperts, R.; Stratmann, R. E.; Yazyev, O.; Austin, A. J.; Cammi, R.; Pomelli, C.; Ochterski, J. W.; Ayala, P. Y.; Morokuma, K.; Voth, G. A.; Salvador, P.; Dannenberg, J. J.; Zakrzewski, V. G.; Dapprich, S.; Daniels, A. D.; Strain, M. C.; Farkas, O.; Malick, D. K.; Rabuck, A. D.; Raghavachari, K.; Foresman, J. B.; Ortiz, J. V.; Cui, Q.; Baboul, A. G.; Clifford, S.; Cioslowski, J.; Stefanov, B. B.; Liu, G.; Liashenko, A.; Piskorz, P.; Komaromi, I.; Martin, R. L.; Fox, D. J.; Keith, T.; Al-Laham, M. A.; Peng, C. Y.; Nanayakkara, A.; Challacombe, M.; Gill, P. M. W.; Johnson, B.; Chen, W.; Wong, M. W.; Gonzalez, C.; Pople, J. A. *Gaussian 03*; Gaussian, Inc.: Wallingford, CT, 2004.
(50) Wang, J. M.; Wang, W.; Kollman, P. A.; Case, D. A. *J. Mol. Graphics Modell.* **2006**, *25*, 247.
(51) Case, D. A.; Darden, T. A.; Cheatham, T. E., 3rd; Simmerling, C.; Wang, J.; Duke, R. E.; Luo, R.; Crowley, M.; Walker, R. C.; Zhang, W.; Merz, K. M.; Wang, B.; Hayik, S.; Roitberg, A.; Seabra, G.; Kolossvary, I.; Wong, K. F.; Paesani, F.; Vanicek, J.; Wu, X.; Brozell, S. R.; Steinbrecher, T.; Gohlke, H.; Yang, L.; Tan, C.; Mongan, J.; Hornak, V.; Cui, G.; Mathews, D. H.; Seetin, M. G.; Sagui, C.; Babin, V.; Kollman, P. A. *AMBER11*; University of California: San Francisco, CA, 2008.
(52) Miyamoto, S.; Kollman, P. A. *J. Comput. Chem.* **1992**, *13*, 952.
(53) Darden, T.; Perera, L.; Li, L.; Pedersen, L. *Structure* **1999**, *7*, R55.
(54) Essmann, U.; Perera, L.; Berkowitz, M. L.; Darden, T.; Lee, H.; Pedersen, L. G. *J. Chem. Phys.* **1995**, *103*, 8577.
(55) Sagui, C.; Pedersen, L. G.; Darden, T. A. *J. Chem. Phys.* **2004**, *120*, 73.
(56) Shirts, M. R.; Mobley, D. L.; Chodera, J. D.; Pande, V. S. *J. Phys. Chem. B* **2007**, *111*, 13052.
(57) Uberuaga, B. P.; Anghel, M.; Voter, A. F. *J. Chem. Phys.* **2004**, *120*, 6363.
(58) Izaguirre, J. A.; Catarello, D. P.; Wozniak, J. M.; Skeel, R. D. *J. Chem. Phys.* **2001**, *114*, 2090.
(59) Larini, L.; Mannella, R.; Leporini, D. *J. Chem. Phys.* **2007**, *126*, 104101.
(60) Loncharich, R. J.; Brooks, B. R.; Pastor, R. W. *Biopolymers* **1992**, *32*, 523.
(61) Aqvist, J. *J. Phys. Chem.* **1990**, *94*, 8021.
(62) Steinbrecher, T.; Mobley, D. L.; Case, D. A. *J. Chem. Phys.* **2007**, *127*, 214108.
(63) Wang, Z.-X.; Wu, C.; Lei, H.; Duan, Y. *J. Chem. Theory Comput.* **2007**, *3*, 1527.
(64) Oostenbrink, C.; Villa, A.; Mark, A. E.; Van Gunsteren, W. F. *J. Comput. Chem.* **2004**, *25*, 1656.
(65) Jorgensen, W. L.; Maxwell, D. S.; Tirado-Rives, J. *J. Am. Chem. Soc.* **1996**, *118*, 11225.